8.1 INTRODUCTION

Intestinal absorption is prerequisite for enhancing bioavailability administered by the peroral route. Various mechanisms are involved in intestinal absorption and can majorly influence its magnitude including permeation of the intestinal mucosa by passive diffusion, carrier mediated transport across intestinal wall, enzymatic and chemical alteration of the molecule in the intestinal lumen and/or in the enterocyte, dissolution behavior of the drug and interaction with food ingredients or co-administered drugs at the dissolution and the transport level. Despite of having recent advances, a complex process of intestinal absorption is fundamentally still poorly understood. Therefore, experimental verification of drug absorption is carried out in the industrial drug development practice. Prediction of in vivo absorption based on in vitro methodology may help in reducing the volume of necessary clinical investigations. Caco-2 cell line is predominantly used as a tool to study intestinal absorption in the last decade (1).

Various in vitro methods are listed in United States FDA guidelines to evaluate the permeability of a drug molecule, includes monolayer of suitable epithelial cells. Currently there is substantial interest in development of cell culture systems that would mimic the intestinal mucosa in order to evaluate strategies for investigating and/or enhancing drug absorption. The intestinal epithelial cells of primary interest, from the standpoint of drug absorption and metabolism, are the villus cells, which are fully differentiated cells. Caco-2 cell line consists of a monolayer of differentiated villus cells similar to that of small intestine which represents a potential tool in the study of drug transport and metabolism (2).

In the intestine, a single layer of epithelial cells covers the inner intestinal wall and forms the rate-limiting barrier to the absorption of dissolved drugs. As a consequence, the proper reconstitution of a human differentiated epithelial cell monolayer in vitro allows the prediction of oral drug absorption in humans. The human colon carcinoma cell line Caco-2 has been found to serve this purpose well. The human intestinal Caco-2 cell line differentiates spontaneously in culture without supplementation of differentiating factors and has been extensively used as a model of the intestinal barrier for in vitro toxicology studies (3). The human epithelial colorectal adenocarcinoma cell line, Caco-2 is typically used to represent the predominant cell type in the gut, the gut epithelial cells (4). In culture, this cell line slowly differentiates into monolayers with a differentiated phenotype with many functions of the small intestinal villus epithelium.

Caco-2 cells grown on permeable filters have, therefore, become the golden standard for in vitro prediction of intestinal drug permeability and absorption (5).

The Caco-2 cell line exhibits a well-differentiated brush border on the apical surface and tight junctions. It expresses typical small-intestinal microvillus hydrolases and nutrient transporters. It has proven to be the better in vitro model to study intestinal absorption due to following reasons (5):

a) to elucidate drug transport pathways (e.g., passive, carrier mediated etc.)
b) to assess cellular permeability of drug molecules
c) to determine formulation strategies designed to enhance membrane permeability
d) to assess the physicochemical characteristics for passive diffusion of drugs
e) to evaluate potential toxic effects of drug molecules or formulation components on the biological barrier.

The objective of the present study was to evaluate cytotoxicity, quantitative and qualitative cellular uptake, transport mechanism and permeability of all formulations (AM-SLNs, LH-SLNs, AM-SMEDDS, LH-SMEDDS) in the Caco-2 cell system.

8.2 MATERIALS

Asenapine maleate (AM) and Lurasidone HCl (LH) were received as a gift samples from Alembic Pharmaceuticals Ltd., Vadodara, India. Caco-2 cells were purchased from National Centre for Cell Science (NCCS), Pune, India. Minimum Essential Medium Eagle (MEM), Hank's Balanced Salt Solution (HBSS), Penicillin-streptomycin solution, Trypsin-EDTA solution, Fetal bovine serum (FBS) were purchased from Himedia, Mumbai, India. 12-well Transwell inserts were purchased from Nunc, Denmark. 6, 24 and 96 well plates were purchased from Costar, Corning, USA. Cycloheximide, Sodium azide, Chlorpromazine, Nystatin, Coumarin-6 and MTT dye were purchased from Sigma Aldrich, Mumbai, India.

8.3 METHODS

8.3.1 Culture of Caco-2 cells

Caco-2 cell lines were obtained from the National Centre for Cell Science (NCCS, Pune, India) and the cells of passages 30–40 were used in this study. Caco-2 cells were grown in the tissue culture flasks (75 cm^2), and maintained under 37°C with 5% CO_2 in Jouan IG0150 incubator (Thermo-Fischer, Waltham, USA) to simulate the physiological conditions. The growth medium comprised of Minimum Essential

Medium (MEM), 20% Fetal Bovine Serum (FBS), 100 IU/ml of penicillin and 100 µg/ml of streptomycin. The growth medium was changed on every alternate day with fresh medium for providing optimum nutrients to the cells. The culture cells were trypsinized employing 0.25% trypsin-EDTA solution, once 90% confluent. The harvested cells were then used for subsequent studies (6).

8.3.2 Method of preparation of dye loaded formulations

Dye loaded formulations (Solid lipid nanoparticles (SLNs) and self-microemulsifying drug delivery system (SMEDDS)) were prepared using Coumarin-6 as a hydrophobic model dye.

Coumarin-6 loaded SLNs were formulated by high speed homogenization followed by sonication method adopted for AM-SLNs, by replacing AM with Coumarin-6.

Coumarin-6 loaded SLNs were formulated by high pressure homogenization method adopted for LH-SLNs, by replacing LH with Coumarin-6.

Coumarin-6 loaded SMEDDS were prepared using method adopted for SMEDDS by replacing AM and LH with Coumarin-6.

8.3.3 Cell Viability Assay

The cytotoxicity of SLNs and SMEDDS against Caco-2 cells was assessed by performing 4,5-(dimethylthiazol-2-yl) 2,5-diphenyl-tetrazolium bromide (MTT) assay. This test evaluates the mitochondrial function as a measurement of cell viability, which allows the detection of dead cells before they lose their integrity and shape. The cells were seeded onto 96-well plates at a concentration of 1×10^4 cells/well. Plates were incubated at 37 °C in humidified CO_2 (5%) incubator for 24 h (7). Then, cells were treated with different samples in culture medium (100 µL) at different concentrations in the range of 10-700 µg/ml (8). After 24 h of incubation, the supernatants of each well were removed and the cells were incubated for 4 h with 100 µL of MTT reagent (1 mg/ml) in a serum free MEM. MTT was removed and the formed insoluble formazan crystals were dissolved in 100 µL Dimethyl sulfoxide (DMSO) solution and the optical density measured at 570 nm using Microplate Reader (680-XR, Bio-Rad Laboratories, France). The amount of formazan present is proportional to the number of viable cells, as only living cells will reduce MTT to blue formazan. The results were expressed as a percentage of the absorbance present in the samples treated cells compared to the control cells. Untreated cells were taken as control with 100% viability and cells without addition of MTT were used as blank to calibrate the spectrophotometer to zero

absorbance (7,9-10). Experiments were performed in triplicates (n = 3). The percentage viability was calculated using the following equation:

$$\%viability = \frac{Absorbance\ of\ test}{Absorbance\ of\ control} * 100 \ldots\ldots\ldots\ldots\ldots Equation\ 8.1$$

8.3.4 Intracellular uptake study by Caco-2 cells using confocal microscopy

Cells were seeded at a density of 1×10^6 cells/well on rounded cover slips in 6 well plates for 24 h and allowed to adhere for 24 h. After 24 h, cells were washed with fresh medium and were incubated with 100 µl containing 100µg/ml of Coumarin-6 solution and Coumarin-6 loaded formulations. To investigate time dependent uptake, the cells were incubated with dye loaded formulations (SLNs and SMEDDS) and plain dye solution for 1 h and 4 h. Then, cell monolayers were fixed with 70% ethanol for 20 min and rinsed with PBS. After rinsing, the nuclei were counter-stained with DAPI for 3 min and rinsed again with Hank's Balanced Salt Solution (HBSS), mounted in glycerol and observed using Carl Zeiss confocal laser microscope ((Coumarin: 430 nm excitation and 485 nm emission wavelength, Green fluorescence) and (DAPI: 350 nm excitation and 470 nm emission wavelength, Blue fluorescence)). The images were analyzed by Zen imaging software (11-15).

8.3.5 Intracellular uptake study by Caco-2 cells using flow cytometry

For the flow cytometry, cells were seeded at density of 1×10^5 Caco-2 cells per well in 6-well plate and allowed to adhere for 24 h. After 24 h, cells were co-incubated with 1 ml MEM containing 100 µl containing 100µg/ml of Coumarin-6, Coumarin-6 loaded formulations (SLNs and SMEDDS) for 1 h and 4 h. Cells treated with only medium were used as respective controls. At the end of the incubation period, the cells were washed three times with PBS to eliminate excess of dye and then detached from plates by trypsinization. Cells were collected by centrifugation at 800 rpm for 5 min and supernatant was discarded. The cells were resuspended in fluorescence-activated cell sorting (FACS) buffer (PBS + 1%BSA (Bovine Serum Albumin) +1%FBS) and fluorescence was measured in FACS (FACS Canto-II, BD Biosciences, San Jose, CA, USA) using software provided with the instrument (BD FACS Diva 6.1.3 software, BD Biosciences, San Jose, CA, USA). For each sample, 10000 events were collected (14-18).

8.3.6 Uptake mechanism elucidation of SLNs in Caco-2 cell monolayer

The cellular uptake of SLNs in Caco-2 cell monolayers was investigated to clarify its absorption mechanism. The endocytosis of SLNs was investigated using different types of inhibitors, such as sodium azide (a specific endocytosis inhibitor), chlorpromazine (an inhibitor of receptor mediated and clathrin mediated endocytosis), nystatin (claveole/lipid raft mediated endocytosis). To identify the internalization pathway of both SLNs in the Caco-2 cell monolayer, the uptake experiments were done with the treatment of specific inhibitors for different types of endocytosis (8,15,19).

Caco-2 cells were seeded at density of 1×10^5 cells/well were on 6-well plate and allowed to attach and grow. Cell monolayers were first incubated with freshly replaced culture medium containing sodium azide (0.1% w/v), chlorpromazine (10 μg/ml) and nystatin (50 μg/ml) for 1 h at 37°C. After 1 h, SLNs (10 μg/ml) were added into the inhibitor solution and co-incubated for 2 h. At the end of incubation period, cells were lysed using 1% Triton X-100 (8,15,19). Drug was extracted from the lysate with acetonitrile and quantified by HPLC as described in section 3.3 and 3.6.

8.3.7 Permeability study across Caco-2 monolayer using Transwell permeable insert

Caco-2 cells suspension was seeded at the density of 5000 cells/well on 12 mm Transwell polycarbonate membrane inserts with 0.4 mm pores and cultured for 21 days. The volume of cell suspension in complete growth media used was 0.1 ml. In the basolateral side, 0.5 ml of complete growth media was added. Growth media from both sides were removed and replaced every 2 d for 21 d until cells were confluent (8,13,20). The integrity of the cell monolayer was checked once every week starting at day 4 and then at day 21 post seeding, as well as at the beginning and the end of each absorption experiments by measuring the trans epithelial electrical resistance (TEER) using EVOM2 (World Precision Instrument, Sarasota, FL, USA). In addition, absorption of Lucifer yellow across the cell layer was determined at the end of each experiment as a control.

The permeability of formulations (SLNs and SMEDDS) across intestinal in vitro models was evaluated by comparing drug suspension with drug loaded formulations, in Caco-2 cells. Those monolayers with TEER more than 800 $\Omega\bullet cm^2$ were used in the transport studies. The integrity of the monolayers was also checked by monitoring the permeability of the paracellular leakage marker, Lucifer yellow across the monolayers. The cell monolayers were considered tight enough for the transport experiments when

the apparent permeability coefficient (Papp) for Lucifer yellow was less than 0.5×10^{-6} cm/s (5).

For apical to basolateral transport study, 0.5 ml containing 100 µg/ml each SLNs and SMEDDS diluted with transport medium (100 µg/ml) was added to apical side, while 0.5 ml of drug suspension (100 µg/ml) in transport medium (HBSS) was added as the control. The basolateral side of the inserts contained 1.5 ml volume of transport buffer. After incubation for 30, 60, 120, 180 and 240 min, aliquot of 100 µl was withdrawn from the receiver chambers and was immediately replenished with an equal volume of pre-warmed HBSS. The amount of drug permeated was determined by HPLC analysis as described in section 3.4 and 3.7 ((8,13,20). The apparent permeability coefficient (Papp) was determined from the linear slope of the plot using the following equation:

$$P_{app} = \frac{dQ}{dt}\frac{1}{A\,C_0} \ldots\ldots\ldots\ldots\ldots\ldots\ldots\ldots Equation\ 8.2$$

where, P_{app} is the apparent permeability coefficient (cm/s), dQ/dt is the steady state flux, A is the surface area of membrane (cm^2), C_0 is the initial concentration of drug taken.

Enhancement ratio (ER) was calculated using following formula:

$$ER = \frac{P_{app}\ of\ formulation}{P_{app}\ of\ drug\ suspension} \ldots\ldots\ldots\ldots Equation\ 8.3$$

8.4 RESULTS AND DISCUSSION

8.4.1 CELL VIABILITY ASSAY

Toxicology of nanomaterials is becoming an important issue nowadays, especially with regard to nanomaterials present in environment and nanomaterials intended for medical use (21). Intracellularly, nanomaterials may interact with cellular components, disrupt or alter cell function, or create reactive oxygen species (ROS). Interactions of nanomaterials with the mitochondria and cell nucleus are being considered as main sources of toxicity (22,23). The currently available data appear to confirm that the SLNs satisfy many prerequisites for being a well-tolerated nanocarrier. Approval for use in pharmaceutical products will require more evidence regarding the safety of the SLNs (21,24). Consequently, the cytotoxicology of the SLNs and SMEDDS in the Caco-2 cell line was systematically investigated in the present study. Moreover, this study will also help in selecting concentration range required to be used for further studies.

MTT is a yellow tetrazolium salt that is oxidized by the mitochondrial dehydrogenase in living cells to give a dark blue formazan product. Damaged or dead cells show reduced or no dehydrogenase activity.

8.4.1.1 Asenapine maleate (AM) loaded SLNs and Asenapine maleate suspension

The results of cell viability assay of blank SLNs, AM-SLNs and AM suspension are shown in figure 8.1. It is reported that cell viability of 70% and less is to be considered as a cytotoxic effect (24).

The cell viability did not decrease significantly with AM suspension (>80%) indicating AM was non-toxic. The results showed 100% cell viabilities with blank SLNs upto 100 µg/ml concentration for 4 h indicating the carrier used for SLNs itself was non-toxic (Figure 8.1). Moreover, greater than 70% of cell viability was observed upto 300 µg/ml. Further increase in concentration significantly reduced cell viability. AM-SLNs also showed >70% cell viability upto 300 µg/ml. Increasing concentration from 300 µg/ml to 500 µg/ml reduced cell viability. No significant difference was observed in cell viabilities of blank and drug loaded SLNs. Hence, it can be said that AM was non-toxic.

The results demonstrated absence of any cytotoxic effects of AM-SLNs upto 100 µg/ml concentration. Hence, 100 µg/ml was the maximum concentration used for uptake and permeation studies (21,24).

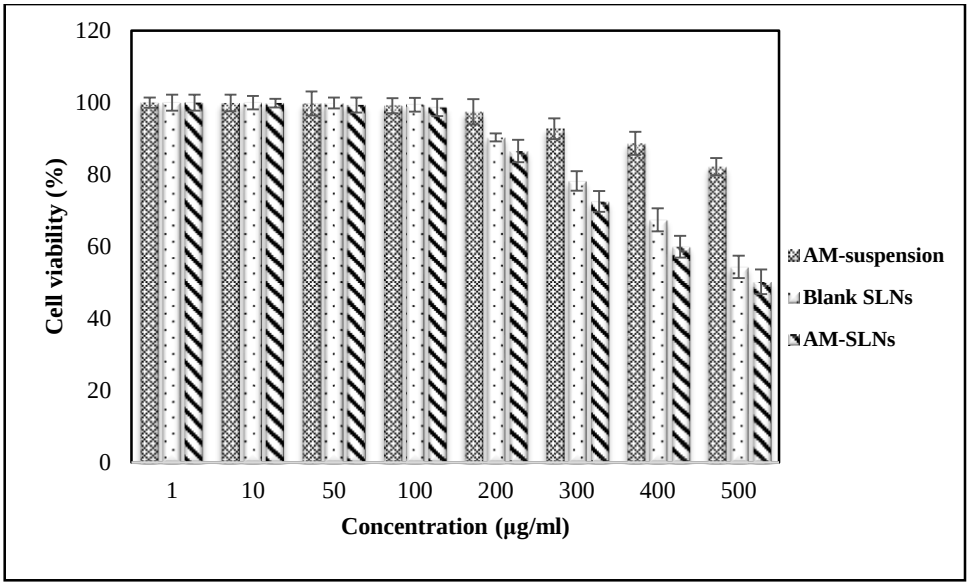

Figure 8.1: Cell viability assay of the AM-SLNs in Caco-2 cell line

8.4.1.2 Lurasiodne hydrochloride (LH) loaded SLNs and Lurasiodne hydrochloride suspension

The results of cell viability assay of blank SLNs, LH-SLNs and LH-suspension are shown in figure 8.2.

LH suspension showed cell viability >80% indicating drug itself had no any toxic effect on Caco-2 cells. The cell viabilities did not significantly decrease after incubation upto 100 µg/ml of blank SLNs for 4 h indicating the carrier used for SLNs itself was non-toxic. Further increase in concentration from 100 µg/ml to 300 µg/ml reduced cell viability. LH-SLNs were found to be safe till 100 µg/ml concentration. There was no significant difference in cell viabilities of blank and drug loaded SLNs. Hence, 100 µg/ml was the maximum concentration used for further studies.

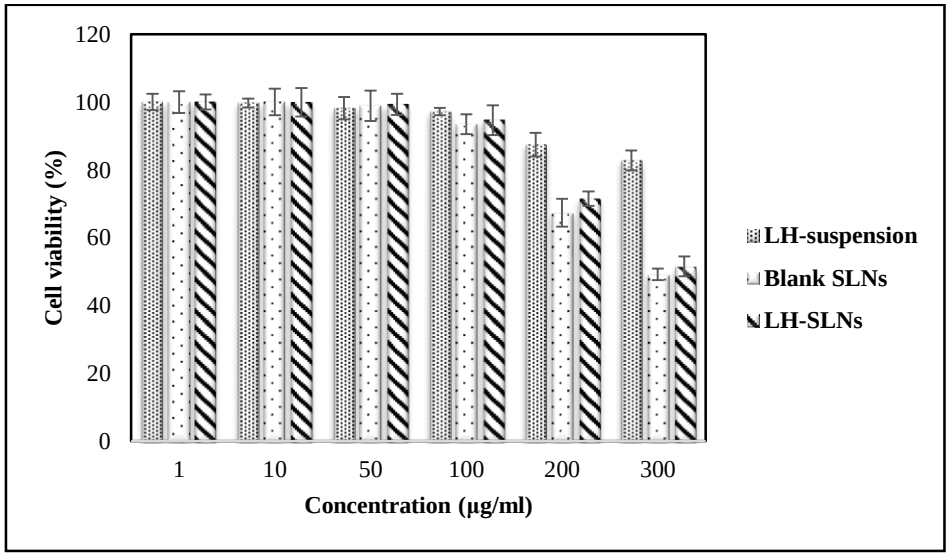

Figure 8.2: Cell viability assay of the LH-SLNs in Caco-2 cell line

8.4.1.3 Asenapine maleate (AM) loaded SMEDDS and Asenapine maleate suspension

It is widely known that a number of surfactant-containing carriers have potential toxicity (9,20,25-27). Therefore, it was necessary to evaluate toxicity of surfactants used in SMEDDS on Caco-2 cells.

In this study, the viabilities of Caco-2 cells incubated with different concentrations of blank SMEDDS, AM-SMEDDS and AM suspension were determined. The MTT assay results are shown in figure 8.3.

The cell viability did not decrease significantly with drug suspension (>80%) indicating AM is non-toxic. Blank SMEDDS showed 100% cell viability upto 100 µg/ml concentration. A concentration-dependent cytotoxicity was observed suggesting that SMEDDS with >150 µg/ml were capable of inducing toxicity on Caco-2 cells. Hence, the proposed working concentration was 100 µg/ml. AM-SMEDDS also showed 100% viability till 100 µg/ml. No significant difference was observed in cell viabilities between blank and AM loaded SMEDDS which inturn confirmed non-toxic effect of AM.

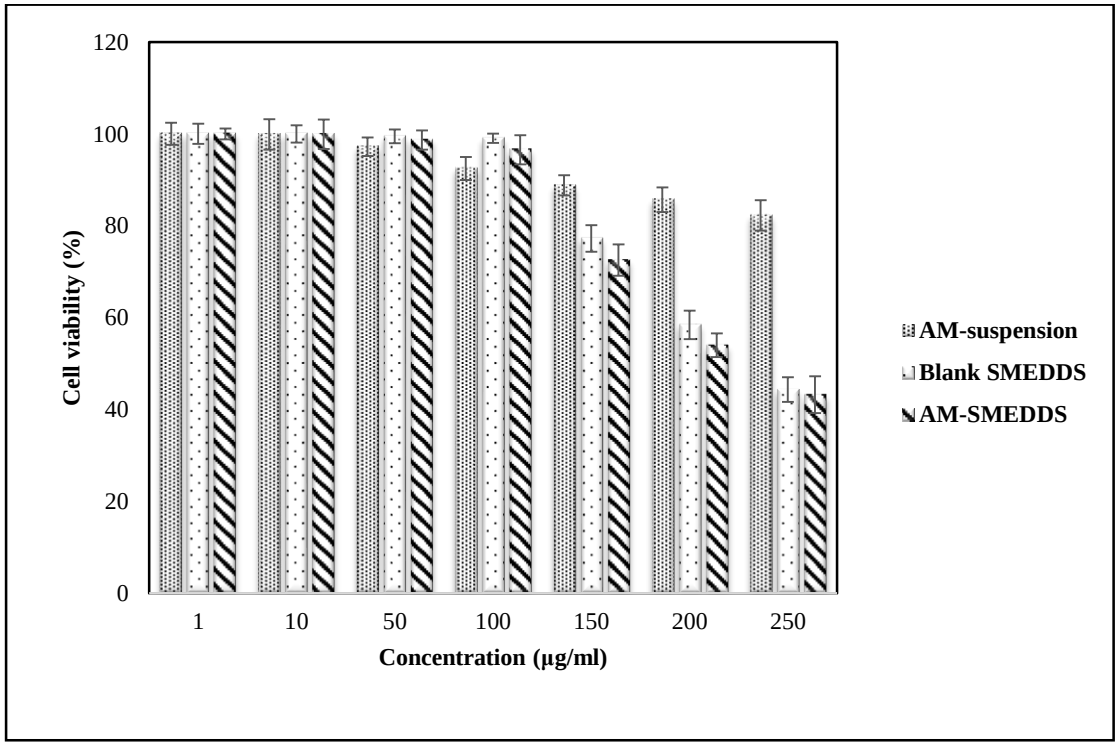

Figure 8.3: Cell viability assay of the AM-SMEDDS in Caco-2 cell line

8.4.1.4 Lurasiodne hydrochloride (LH) loaded SMEDDS and Lurasiodne hydrochloride suspension

In this study, the viabilities of Caco-2 cells incubated with different concentrations of blank SMEDDS, LH-SMEDDS and LH-suspension were determined (Figure 8.4).

LH suspension showed cell viability >80% indicating drug itself had no toxic effect on Caco-2 cells. Blank SMEDDS showed 100% cell viability upto 100 µg/ml concentration. A concentration-dependent cytotoxicity was observed suggesting that SMEDDS with >150 µg/ml were capable of inducing toxicity on Caco-2 cells. Hence, 100 µg/ml concentration was used for further studies. No significant difference was observed in cell viabilities between blank and LH loaded SMEDDS which further confirmed non-toxic effect of LH.

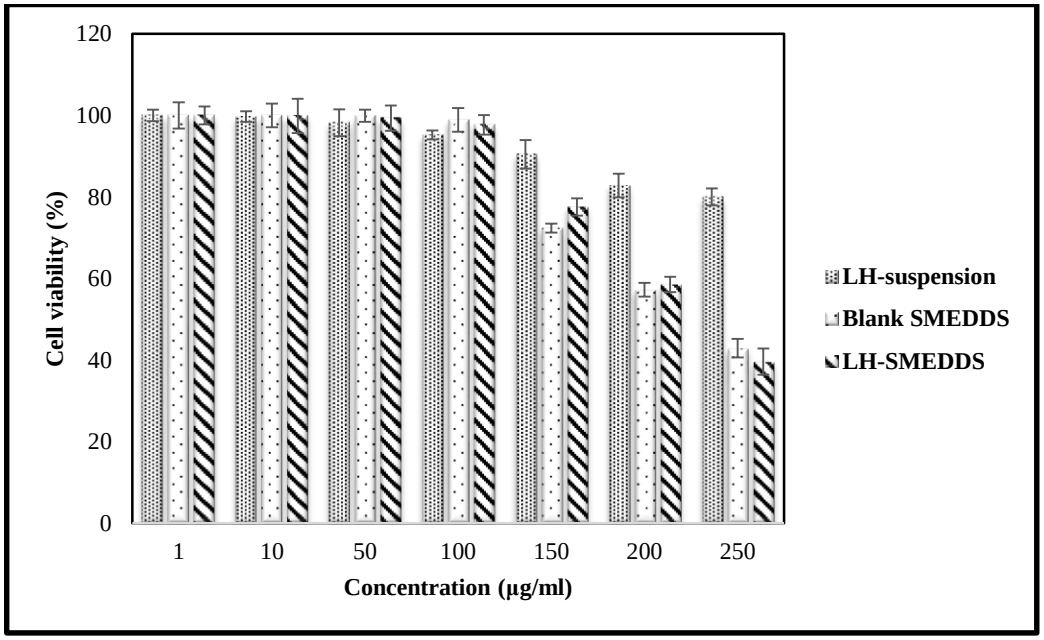

Figure 8.4: Cell viability assay of the LH-SMEDDS in Caco-2 cell line

8.4.2 QUALITATIVE UPTAKE STUDIES USING CONFOCAL MICROSCOPY

The Caco-2 cell line, derived from human colorectal carcinoma, spontaneously differentiates in culture to form confluent monolayers with remarkable morphological and biochemical similarity to the small intestinal epithelium (16). Caco-2 cells have been developed as a useful alternative to animal models to study intestinal absorption of therapeutic agents including proteins, peptides, and oligonucleotides, showing promise that might give useful predictions concerning the oral absorption potential (16,28,29). Therefore, the nanoparticles uptake studies observed in Caco-2 cells could probably be considered to correlate with in vivo situations.

8.4.2.1 Coumarin-6 loaded SLNs, SMEDDS and plain dye solution for Asenapine maleate

This study was conducted to measure the extent of the intracellular transport of the prepared formulations after oral administration. The results of confocal laser scanning of Coumarin-6 solution (control) or Coumarin-6 loaded formulations for AM are illustrated in figure 8.5 to figure 8.11. No fluorescence was detected from the image of the control cells (Figure 8.5a), which were not exposed to the coumarin-6 loaded nanoparticles and/or dye solution, implying there was no auto fluorescence of the cells which can lead to misinterpretation of the data (28,29).

Results indicated that uptake of dye loaded formulations (SLNs and SMEDDS) and dye solution was time dependent. The intensity of the florescence clearly indicated efficient delivery of SLNs and SMEDDS to Caco-2 cells and nucleus appeared blue. It was observed from figure that fluorescence distribution of dye transported across Caco-2 cells was increased with time (Figure 8.6-8.11).

In case of dye solution (Figure 8.6 & 8.7), little uptake was observed and dye was found to be attached to the apical cell surface only at the end of 4 h indicating no internalization of dye solution in Caco-2 cells (24,28,29).

However, both SLNs (Figure 8.8 & 8.9) and SMEDDS (Figure 8.10 & 8.11) showed higher fluorescence intensity, both in the cell cytoplasm as well as in the nucleus at the end of 4 h incubation period implying that nanoparticles were easily internalized into Caco-2 cells. Thus, there was a significant increase in the cellular uptake of both formulations as compared to the dye solution.

The enhanced permeation of SLNs and SMEDDS was attributed to presence of TPGS and Cremophor EL and Trasncutol HP respectively, potential absorption enhancers which may alter epithelial barrier property (25). Hence, enhanced permeation across cell membrane may be due to small particle size and presence of excipients (30-32). It is reported that particles are more efficiently taken up with increasing hydrophobic interactions with the membrane of Caco-2 cells (33). So, it was evident from the results that intracellular uptake of hydrophobic drug (AM) could be enhanced by encapsulating drug in the lipid based nanoformulations.

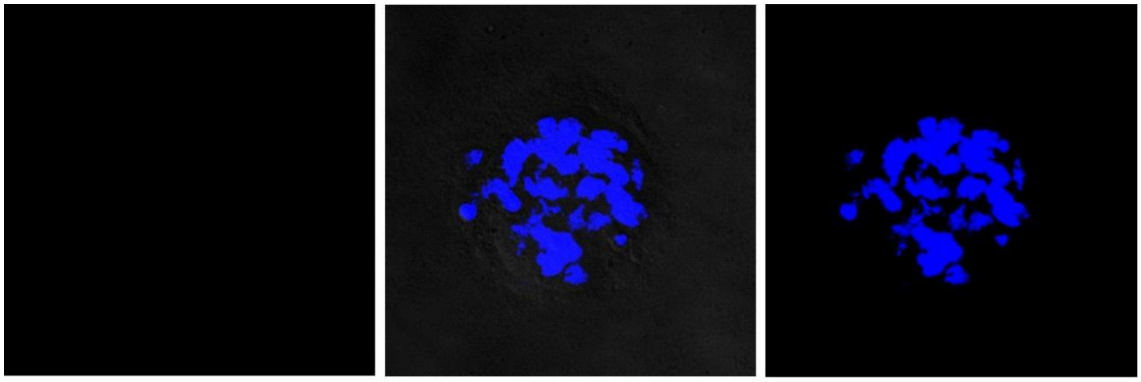

(a) (b) (c)

Figure 8.5 Confocal microscopic images of Caco-2 cells (a) without any treatment (Control) (b) DAPI stained nuclei (c) Overlapped imag

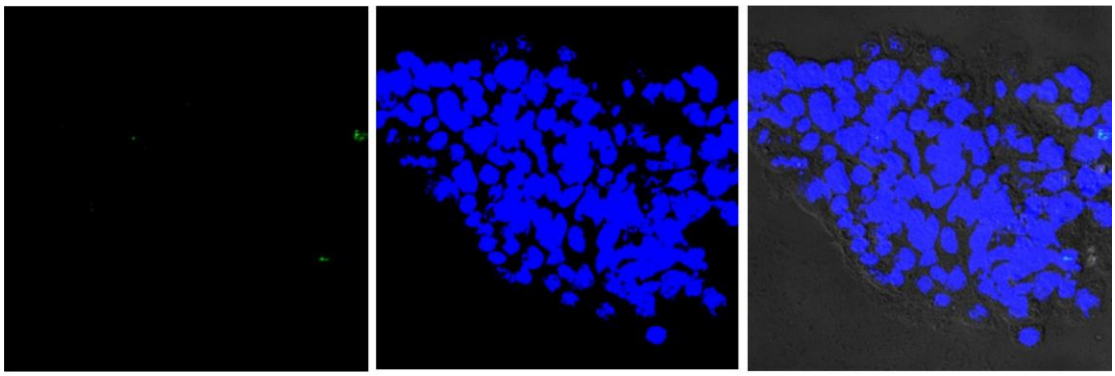

(a) (b) (c)

Figure 8. 6: Confocal microscopic images of Caco-2 cells after 1 h incubation at 37 °C with (a) dye solution (b) DAPI stained nuclei (c) Overlapped image showing no internalization of dye solution in cells for AM

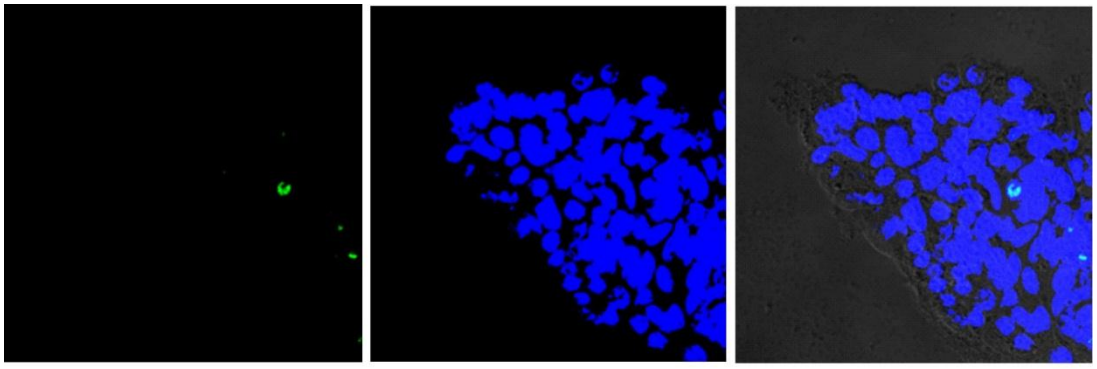

(a) (b) (c)

Figure 8.7: Confocal microscopic images of Caco-2 cells after 4 h incubation at 37 °C with (a) dye solution (b) DAPI stained nuclei (c) Overlapped image showing no internalization of dye solution in cells for AM

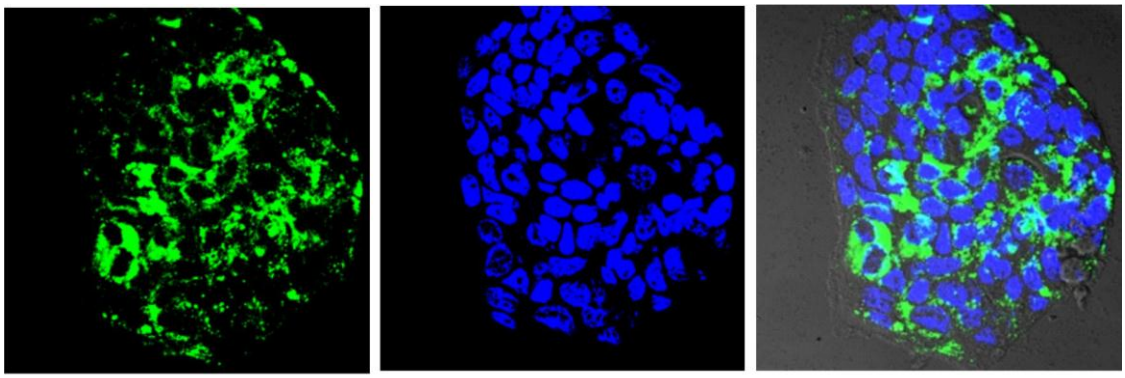

(a) (b) (c)

Figure 8.8: Confocal microscopic images of Caco-2 cells after 1 h incubation at 37 °C (a) 6- coumarin loaded SLNs (b) DAPI stained nuclei (c) Overlapped image showing internalization of SLNs in cells for AM

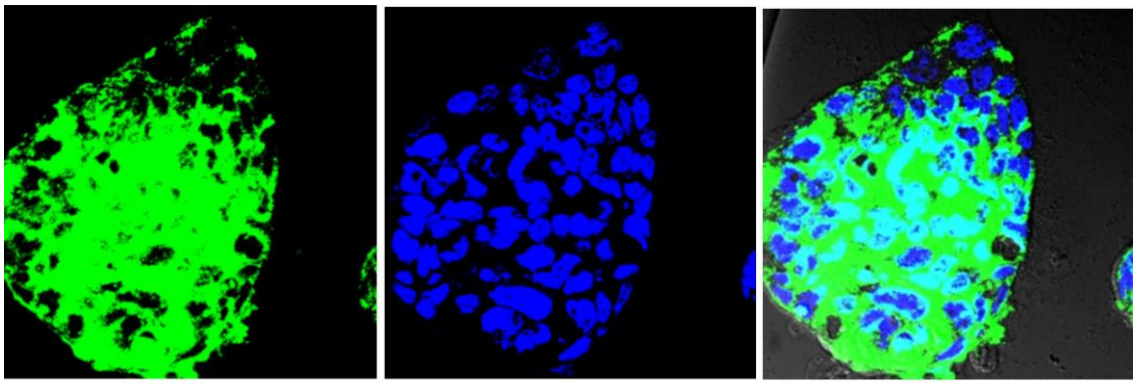

(a) (b) (c)

Figure 8.9: Confocal microscopic images of Caco-2 cells after 4 h incubation at 37 °C with (a) Coumarin-6 loaded SLNs (b) DAPI stained nuclei (c) Overlapped image showing internalization of SLNs in cells for AM

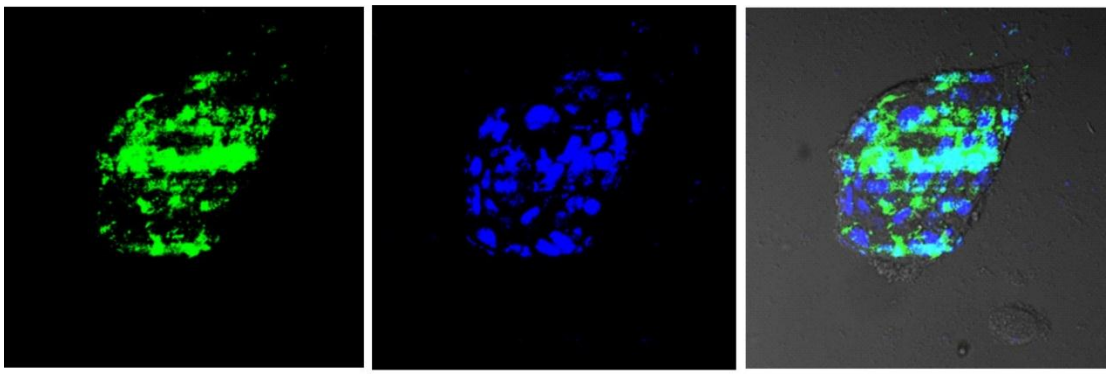

(a) (b) (c)

Figure 8.10: Confocal microscopic images of Caco-2 cells after 1 h incubation at 37 °C with (a) Coumarin-6 loaded SMEDDS (b) DAPI stained nuclei (c) Overlapped image showing internalization of SMEDDS in cells for AM

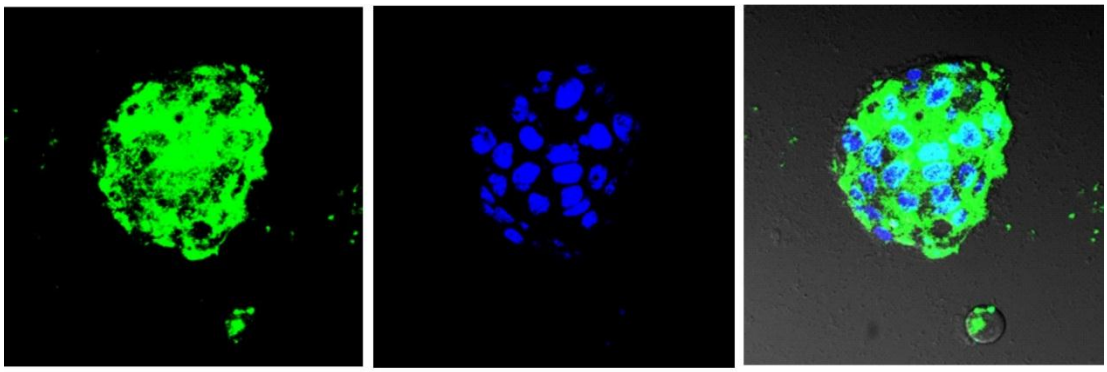

(a) (b) (c)

Figure 8.11: Confocal microscopic images of Caco-2 cells after 4 h incubation at 37 °C with (a) Coumarin-6 loaded SMEDDS (b) DAPI stained nuclei (c) Overlapped image showing internalization of SMEDDS in cells for AM

8.4.2.2 Coumarin-6 loaded SLNs, SMEDDS and plain dye solution for Lurasidone Hydrochloride

The confocal images of Coumarin-6 solution (control) or Coumarin-6 loaded formulations are illustrated in figure 8.12 to figure 8.17. In case of dye solution, little uptake was observed and dye was found to be attached to the apical cell surface only at the end of 4 h indicating no internalization of dye solution in Caco-2 cells (Figure 8.12 & 8.13).

It was clearly demonstrated from the confocal images of Caco-2 cells that both SLNs (Figure 8.14 & 8.15) and SMEDDS (Figure 8.16 & 8.17) showed strong fluorescence intensity, both in the cell cytoplasm as well as in the nucleus at the end of 4 h incubation period implying nanoparticles can be easily internalized into Caco-2 cells as compared to plain dye solution and uptake was time dependent.

The enhanced uptake of SLNs might be due to penetration enhancing effect of sodium deoxycholate present in SLNs. In case of SMEDDS, uptake could be enhanced due to presence of Cremophor EL and Transcutol HP.

It can be evident from the results that intracellular uptake of hydrophobic drug (LH) could be enhanced by encapsulating drug in the lipid based nanoformulations and can lead to enhanced oral bioavailability as hypothesized.

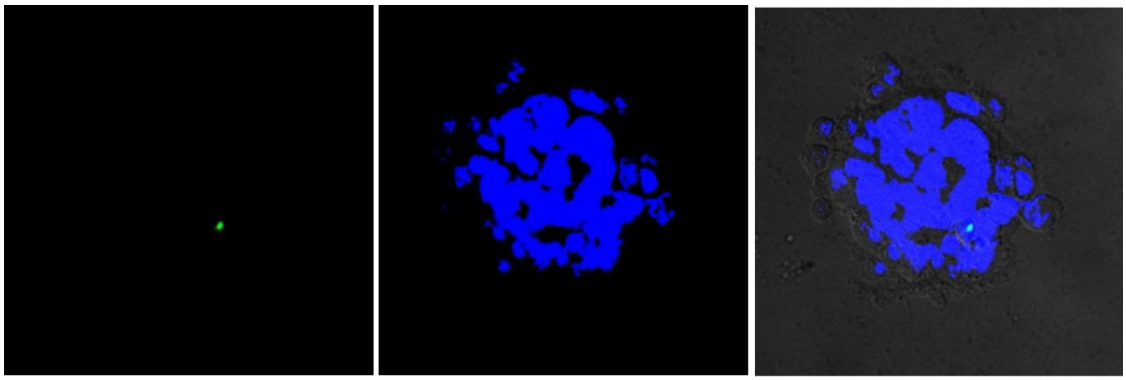

(a) (b) (c)

Figure 8. 12: Confocal microscopic images of Caco-2 cells after 1 h incubation at 37 °C with (a) dye solution (b) DAPI stained nuclei (c) Overlapped image showing no internalization of dye solution in cells for LH

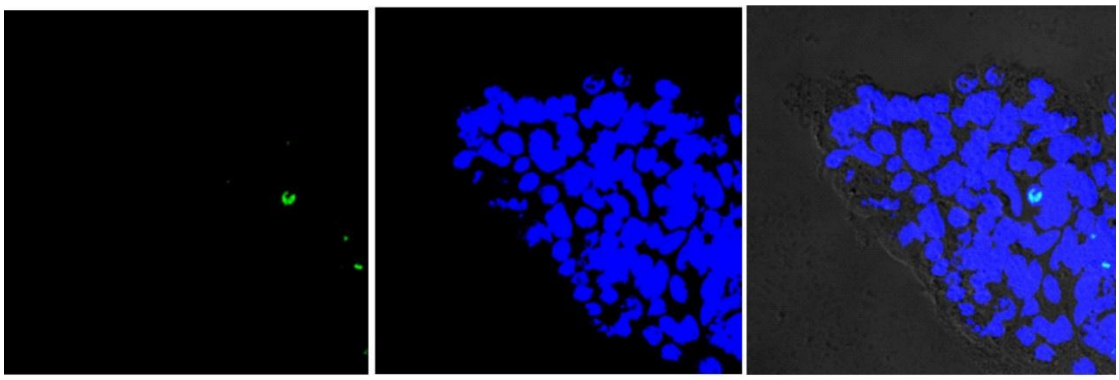

(a) (b) (c)

Figure 8.13: Confocal microscopic images of Caco-2 cells after 4 h incubation at 37 °C with (a) dye solution (b) DAPI stained nuclei (c) Overlapped image showing no internalization of dye solution in cells for LH

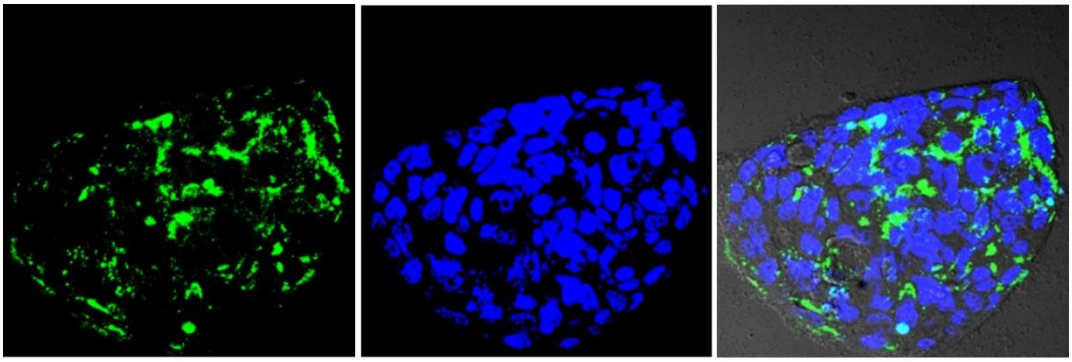

(a) (b) (c)

Figure 8.14: Confocal microscopic images of Caco-2 cells after 1 h incubation at 37 °C with (a) Coumarin-6 loaded SLNs (b) DAPI stained nuclei (c) Overlapped image showing internalization of SLNs in cells for LH

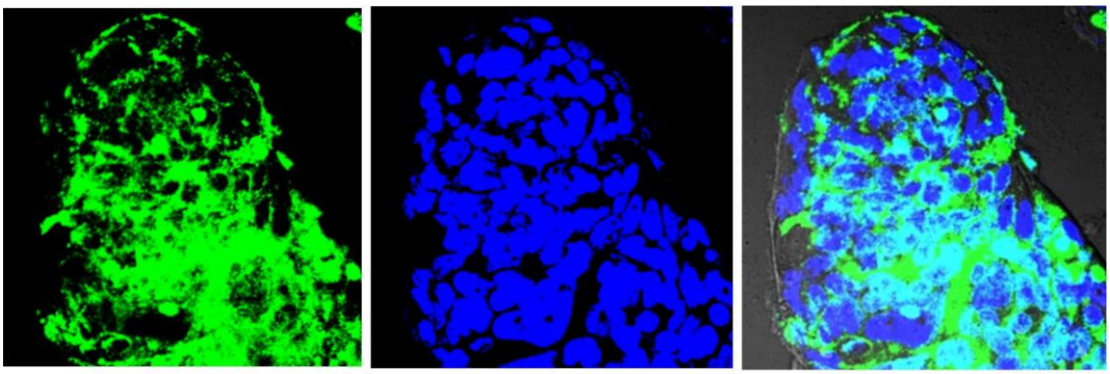

(a) (b) (c)

Figure 8.15: Confocal microscopic images of Caco-2 cells after 4 h incubation at 37 °C with (a) coumarin 6-loaded SLNs (b) DAPI stained nuclei (c) Overlapped image showing internalization of SLNs in cells for LH

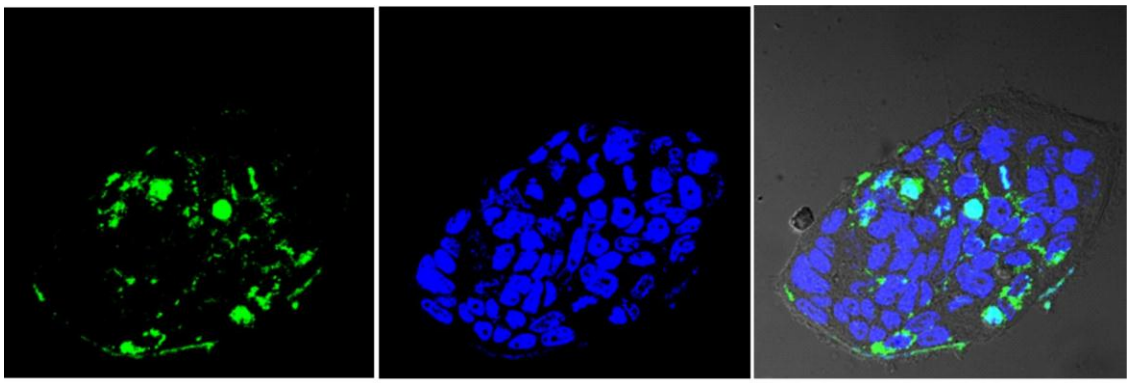

(a) (b) (c)

Figure 8.16: Confocal microscopic images of Caco-2 cells after 1 h incubation at 37 °C with (a) Coumarin-6 loaded SMEDDS (b) DAPI stained nuclei (c) Overlapped image showing internalization of SMEDDS in cells for LH

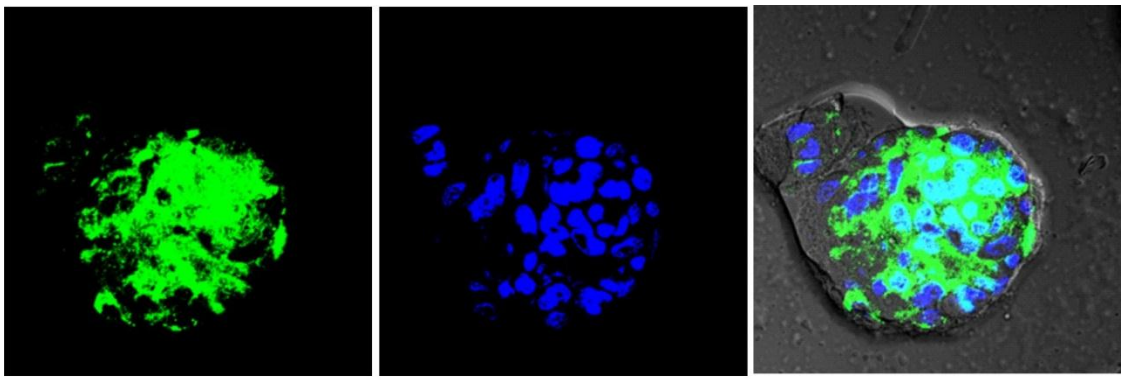

(a) (b) (c)

Figure 8.17: Confocal microscopic images of Caco-2 cells after 4 h incubation at 37 °C with (a) Coumarin-6 loaded SMEDDS (b) DAPI stained nuclei (c) Overlapped image showing internalization of SMEDDS in cells for LH

8.4.3 QUANTITATIVE UPTAKE STUDY USING FLOW CYTOMETRY

8.4.3.1 Coumarin-6 loaded SLNs, SMEDDS and plain dye solution for Asenapine maleate

The quantitative uptake of all formulations by Caco-2 cells were studied using flow cytometry analysis. The relative extent of intracellular uptake of all formulations were calculated using mean fluorescent intensity (MFI).

It was observed that the mean fluorescence intensity inside the cells was significantly increased by Coumarin-6 loaded SLN and SMEDDS as compared to plain dye solution. Flow cytometry analyses revealed that SLNs and SMEDDS in Caco-2 cells were internalized in a time dependent manner and their uptake was significantly increased at the end of 4 h. This uptake was depicted as comparative dot plot analysis (Figure 8.18), mean fluorescence intensity graph (Figure 8.19) and histogram (Figure 8.20).

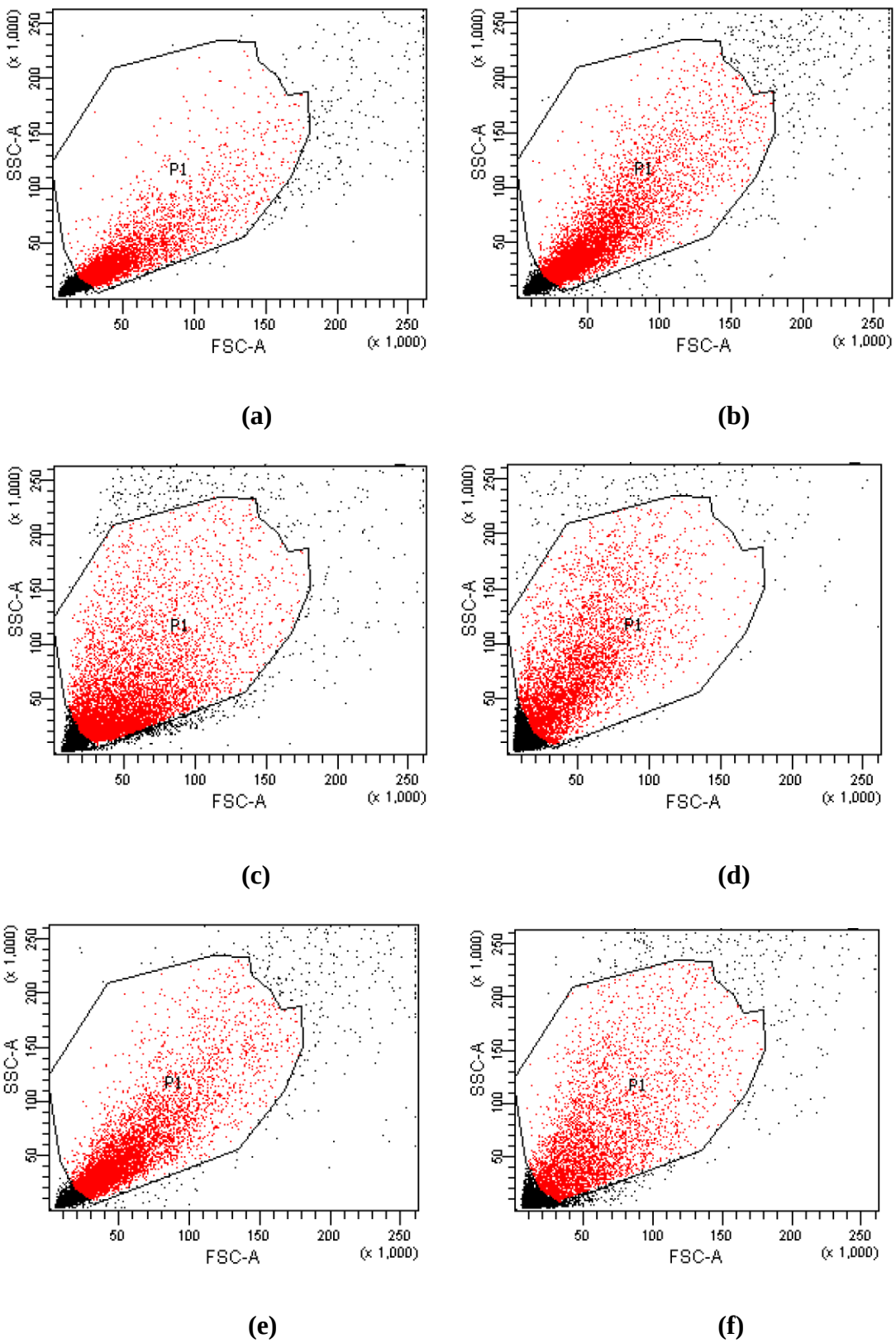

Figure 8.18: Comparative dot plot showing uptake of Coumarin-6 solution, Coumarin-6 loaded SLNs, and Coumarin-6 loaded SMEDDS at 1 h (a,c,e) and 4 h (b,d,f) in Caco-2 cells for AM

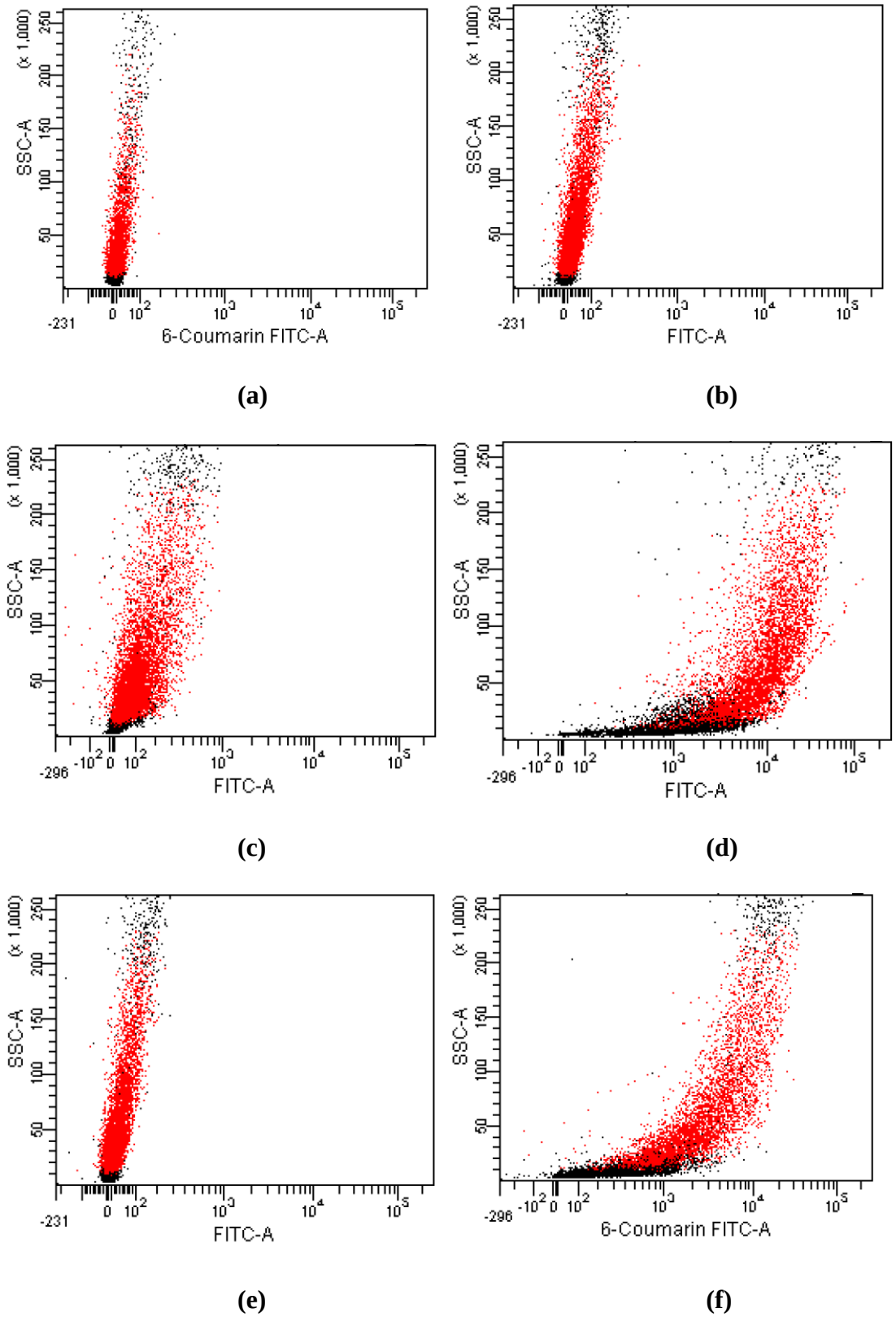

Figure 8.19: Mean fluorescence intensity graph showing uptake of Coumarin-6 solution, Coumarin-6 loaded SLNs, and Coumarin-6 loaded SMEDDS at 1 h (a,c,e) and 4 h (b,d,f) in Caco-2 cells for AM

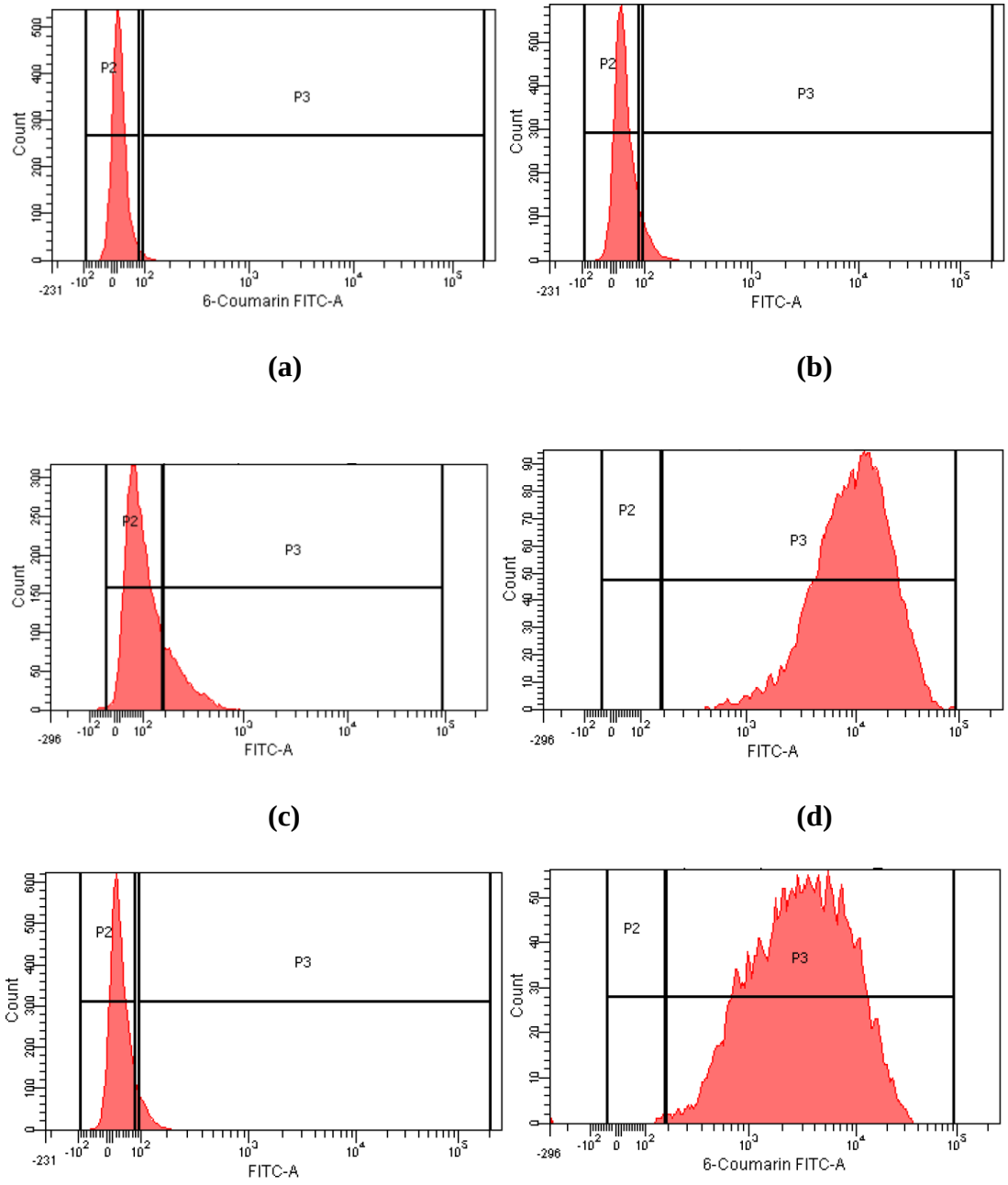

(a) **(b)**

(c) **(d)**

(e) **(f)**

Figure 8.20: Histogram showing uptake of Coumarin-6 solution, Coumarin-6 loaded SLNs, and Coumarin-6 loaded SMEDDS at 1 h (a,c,e) and 4 h (b,d,f) in Caco-2 cells for AM

MFI with Coumarin-6 loaded SLN and SMEDDS was increased 99.24 and 38.90 times with respect to plain dye solution (Figure 8.21). The results of flow cytometry strongly support the previous qualitative measurements of the intracellular uptake of SLNs and SMEDDS for AM by showing significant increase in MFI in the cell cytoplasm as well as in the nucleus as compared to plain dye solution.

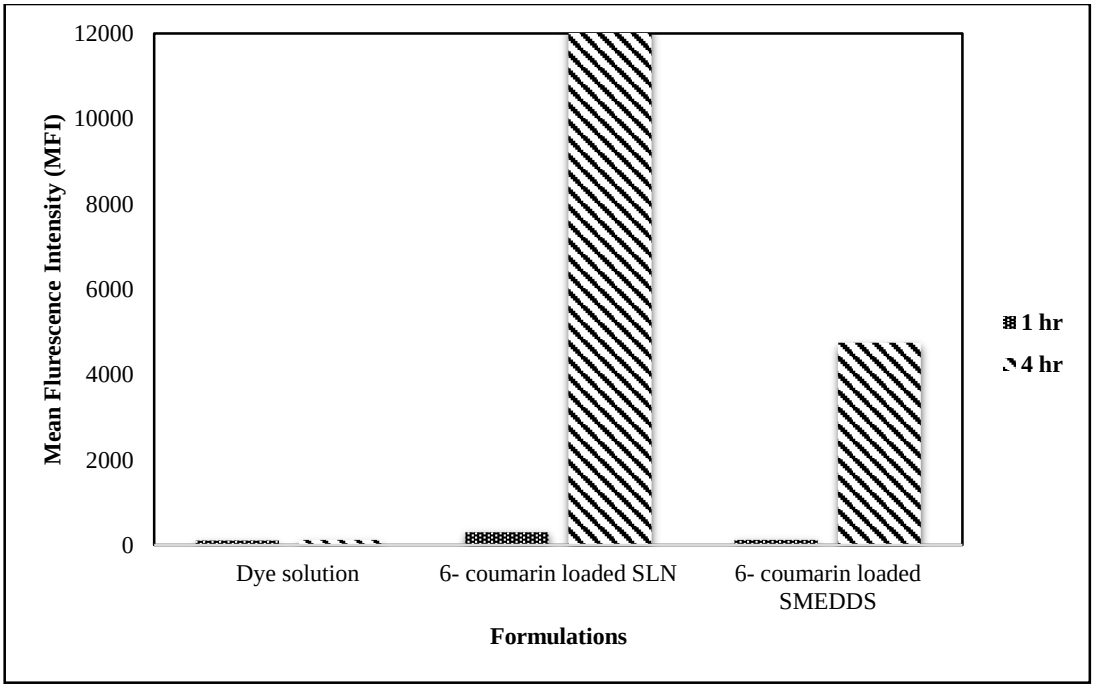

Figure 8.21: Mean fluorescence intensity plot of dye solution, Coumarin-6 loaded SLN and Coumarin-6 loaded SMEDDS for AM

8.4.3.2 Coumarin-6 loaded SLNs, SMEDDS and plain dye solution for Lurasidone hydrochloride

The uptake was depicted as comparative dot plot analysis (Figure 8.22), mean fluorescence intensity graph (Figure 8.23) and histogram (Figure 8.24).

The results confirmed that Coumarin-6 loaded SLNs and Coumarin-6 loaded SMEDDS were internalized in a time dependent manner and their uptake could be increased at end of 4 h. It was observed that the mean fluorescence intensity inside the cells was significantly increased by Coumarin-6 loaded SLNs and Coumarin-6 loaded SMEDDS as compared to plain dye solution.

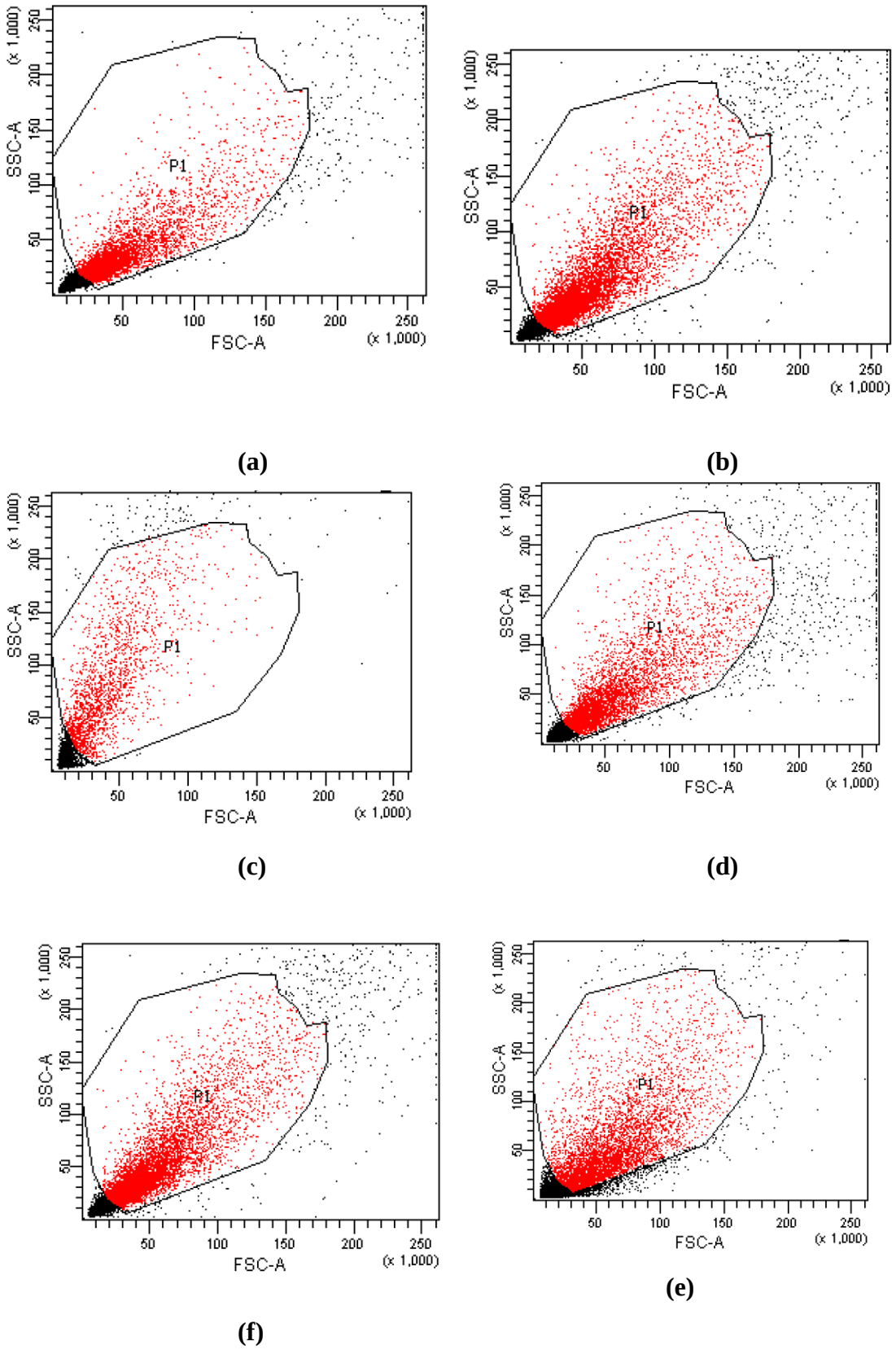

Figure 8.22 : Comparative dot plot showing uptake of Coumarin-6 solution, Coumarin-6 loaded SLNs, and Coumarin-6 loaded SMEDDS at 1 h (a,c,e) and 4 h (b,d,f) in Caco-2 cells for LH

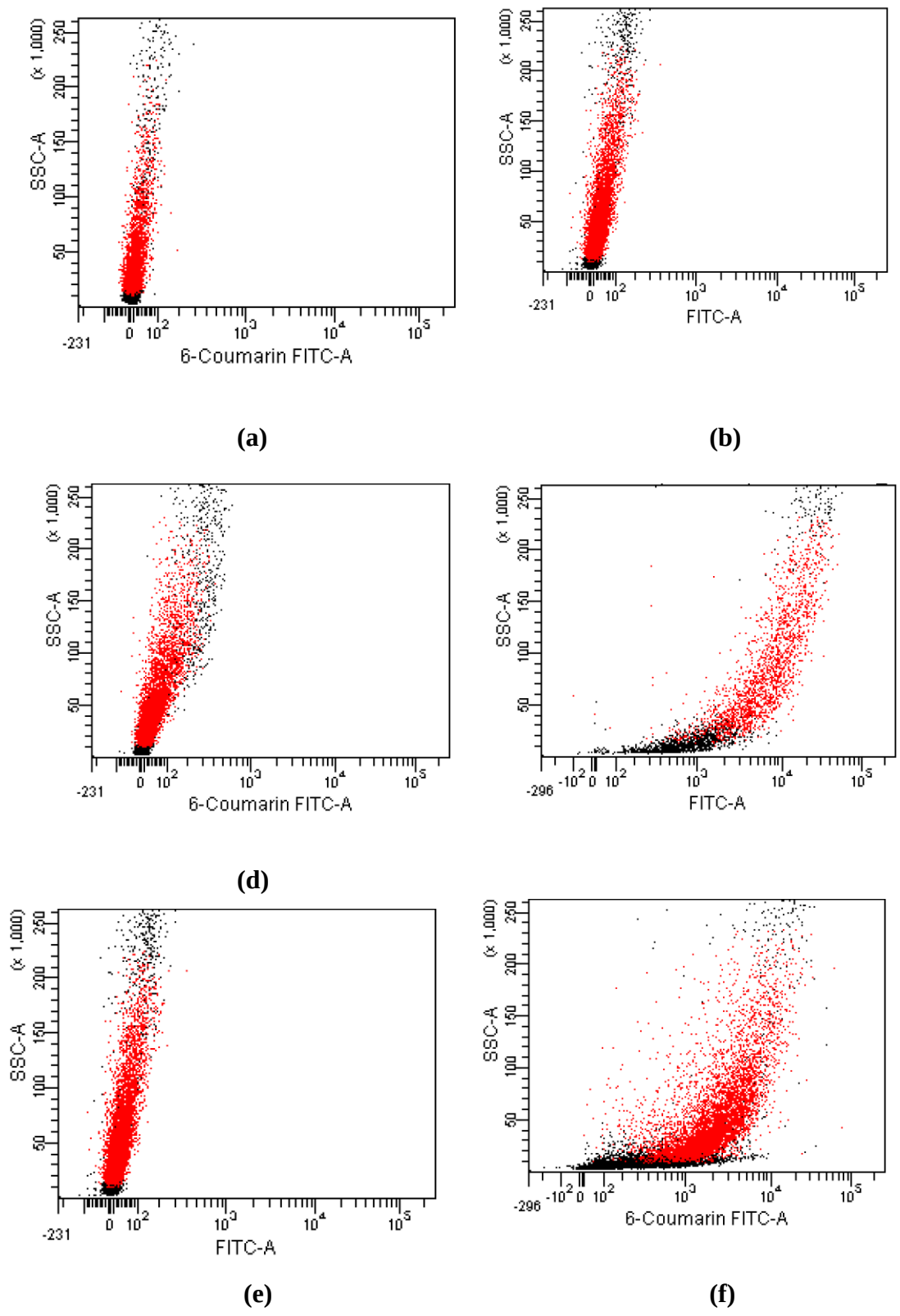

(a) **(b)**

(d)

(e) **(f)**

Figure 8.23 : Mean fluorescent intensity graphs showing uptake of Coumarin-6 solution, Coumarin-6 loaded SLNs, and Coumarin-6 loaded SMEDDS at 1 h (a,c,e) and 4 h (b,d,f) in Caco-2 cells for LH

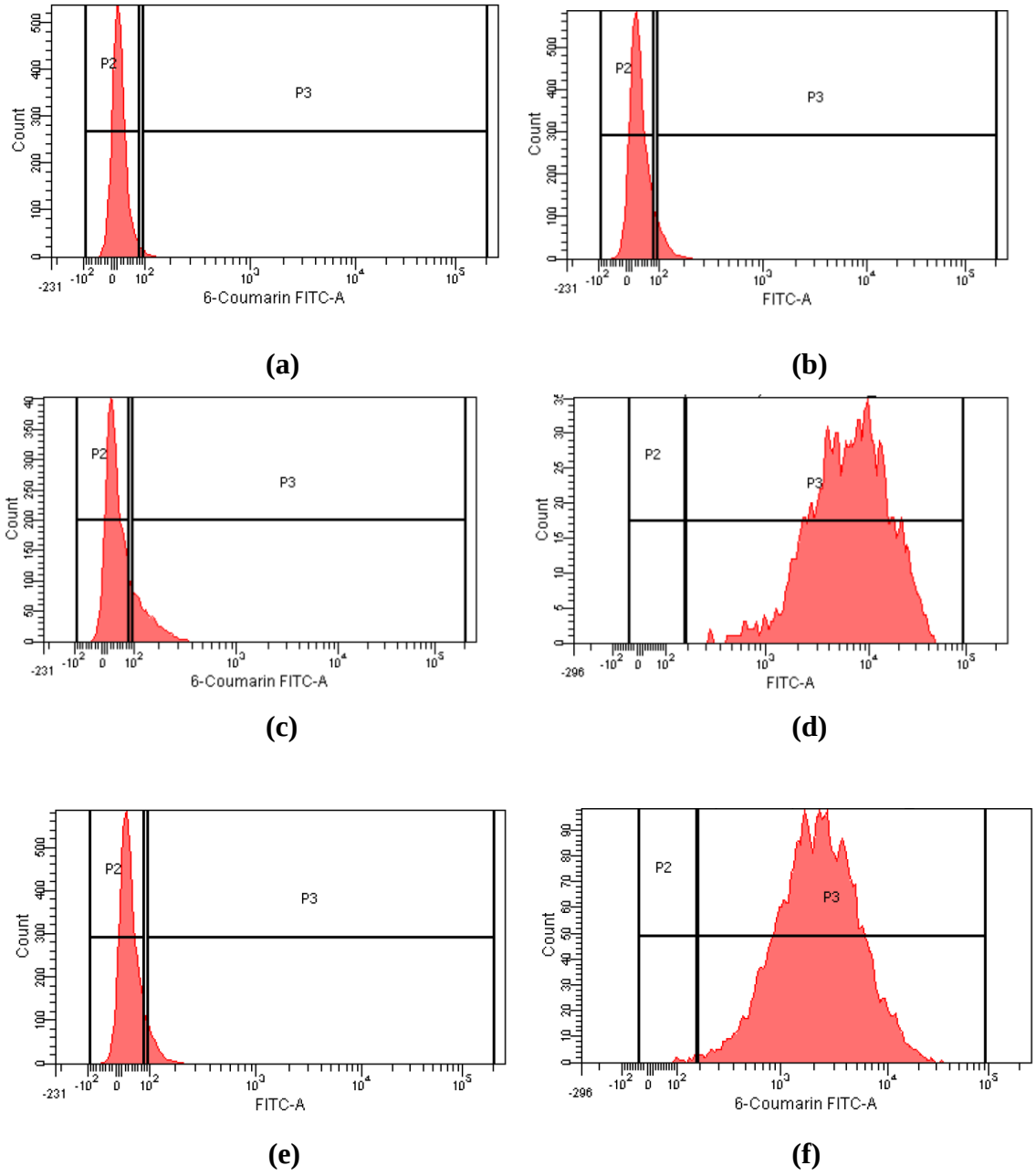

Figure 8.24: Histogram showing uptake of Coumarin-6 solution, Coumarin-6 loaded SLNs, and Coumarin-6 loaded SMEDDS at 1 h (a,c,e) and 4 h (b,d,f) in Caco-2 cells for LH

MFI with Coumarin-6 loaded SLN and SMEDDS was increased 71.71 and 25.57 times with respect to plain dye solution (Figure 8.25). The results of flow cytometry of Caco-2 cells strongly support the previous qualitative measurements of the intracellular uptake of SLNs and SMEDDS for LH by significantly increasing MFI as compared to plain dye solution.

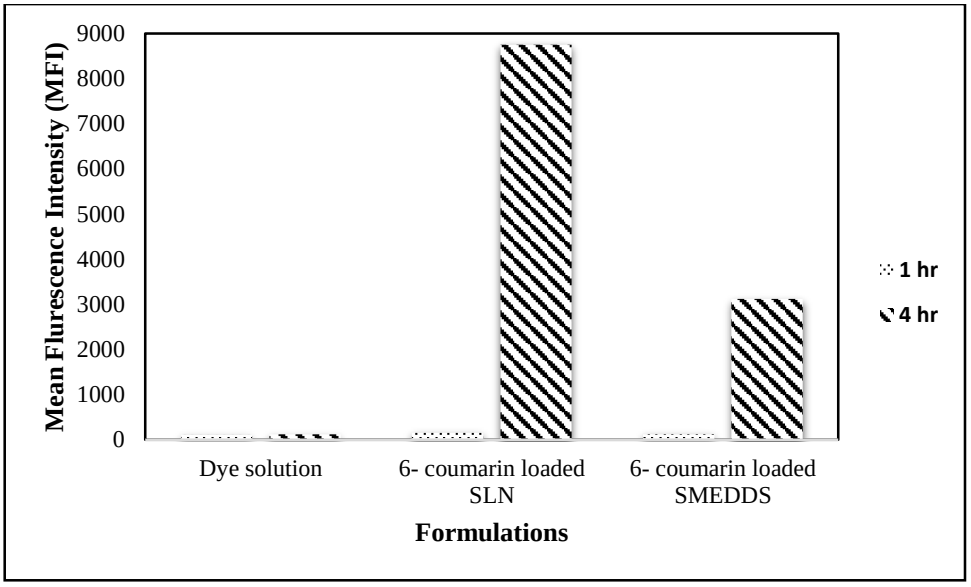

Figure 8.25: Mean fluorescence intensity of dye solution, Coumarin-6 loaded SLN and Coumarin-6 loaded SMEDDS for LH

8.4.4 UPTAKE MECHANISM ELUCIDATION OF SLNS IN CACO-2 CELL MONOLAYER

The objective of the present study was to evaluate the mechanisms of transport of SLNs across Caco-2 monolayer. Although lipid nanoparticles are known to enter into cells in an active endocytic manner, we assessed this phenomenon in Caco-2 cells using sodium azide, an endocytosis inhibitor. The results (Figure 8.26) revealed that intracellular uptake of AM-SLNs and LH-SLNs was only about 13% and 17% of that of normal control in presence of sodium azide. The uptake of AM and LH from their suspension was not reduced in presence of sodium azide. These results allowed us to conclude that SLNs were predominantly internalized by endocytosis, a carrier-mediated process.

Endocytosis has two major routes, phagocytosis and pinocytosis or fluid-phase uptake. Fluid-phase endocytosis, which requires the cargo molecules to be dissolved, can be subdivided into macropinocytosis, clathrin-mediated, caveolin-mediated and clathrin- and caveolin-independent endocytosis (24, 34). Different internalization pathways can be studied in presence of pharmacological (chemical) inhibitors. Hence to evaluate endocytic mechanism of SLNs, transport studies were further undertaken in the presence of different inhibitors and quantified by HPLC (14).

The experimental results suggest that intracellular uptake of both AM-SLNs and LH-SLNs was significantly reduced to 22% and 43% in presence of chlorpromazine and 47% and 56% in presence of nystatin respectively. Thus, it could be deduced that both

clathrin- and lipid raft/caveolae-mediated endocytosis may be involved in the uptake of SLNs across the Caco-2 cell monolayer (18,34,35).

For the different treatment conditions, there is no significant difference in transport of plain drug suspension of AM and LH. This suggest that plain drug solution does not undergo active endocytic uptake mechanism. It can be said that drug suspension is absorbed by passive diffusion process.

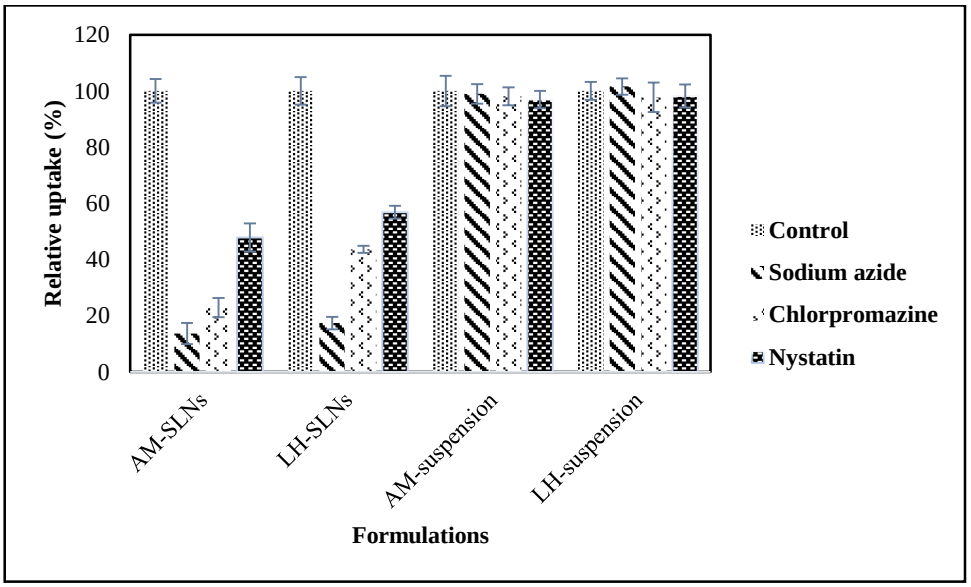

Figure 8.26: Intracellular uptake of SLNs and drug suspension in presence of specific inhibitors

Clathrin mediated endocytosis involves the assembly of a specific coat protein, clathrin, on the intracellular face of the plasma membrane, resulting in the formation of a clathrin coated pit. This pathway is characteristic of receptor-mediated endocytosis; in addition to clathrin, it requires a number of adaptor and accessory molecules for controlling different steps in the assembly and maturation of the coated pits. Among these proteins, a so-called adaptor protein (AP)2 complex is critical for the initial linkages between cargo molecules and clathrin, whereas amphiphysin and dynamin guanosine triphosphatase (GTPase) regulate later conversion of membrane invagination into a vesicle. Chlorpromazine inhibition involves loss of clathrin and adaptor protein 2 complex from the cell surface and their artificial assembly on endosomal membranes which reduces the number of coated pit associated receptors at the cell surface by disrupting the assembly and disassembly of clathrin (34,36-38).

Lipid Raft/Caveolae-Mediated Endocytosis involves invagination of cholesterol-enriched microdomains within the plasma membrane that may contain a coat protein

known as caveolin. These structures are referred to as lipid rafts or caveolae. Lipid raft/caveolae-mediated endocytosis participates in the internalization of glycosylphosphatidylinositol (GPI)- anchored proteins, cholera toxin entry, and intracellular cholesterol trafficking. Nystatin interact with cholesterol in model and biological membranes and are able to change properties of cholesterol rich membrane domains. It creates large aggregates in the membrane and aggregates accumulate cholesterol, thereby sequestering this lipid from the membrane structures. As a result, it induces a profound distortion of the structure and functions of the cholesterol-rich membrane domain, including aberrations in the caveolar shape, dispersion of GPI-anchored proteins from these structures, as well as the inhibition of lipid raft ligands internalization (34,36-38).

So, it was proven that internalization of SLNs involved clathrin- and caveolae mediated endocytosis across Caco-2 cells.

8.4.5 PERMEABILITY STUDY

8.4.5.1 Asenapine maleate (AM) loaded SLNs, SMEDDS and Asenapine maleate suspension

The permeability study using transwell insert was carried out to determine permeability of formulations and drug suspension across Caco-2 cells. The amount of drug transfer from AM-SLNs, AM-SMEDDS and drug suspension across Caco-2 monolayer is shown in table 8.1. It was observed that amount of AM transported across Caco-2 cell monolayer was significantly increased with SLNs and SMEDDS as compared to AM-suspension.

Table 8.1: Drug transfer across the Caco-2 cell line for AM-SLNs, AM-SMEDDS and AM suspension

Time (min)	AM suspension	AM-SLNs	AM-SMEDDS
	Amount of drug transfer (mg)	Amount of drug transfer (mg)	Amount of drug transfer (mg)
30	0.004	0.013	0.012
60	0.006	0.029	0.043
120	0.013	0.071	0.072
180	0.018	0.112	0.102
240	0.024	0.148	0.137

The P_{app} values of AM apical to basolateral side were compared and results are shown in Table 8.2. The results showed that the AM transport through Caco-2 cell monolayer is increased upon encapsulation into SLN as compared to drug suspension. P_{app} of the AM-SLNs and AM-suspension was found to be 6.25×10^{-6} cm/s and 0.89×10^{-6} cm/s, respectively. The transport of AM-SLNs exhibited 7.02 times higher drug permeation than that of AM-suspension at the end of 4 h. Enhanced permeation may also be attributed to presence of TPGS in the formulation. Moreover, contribution of clathrin and claveloe mediated endocytosis in uptake of SLNs may have resulted in increase in permeability of AM loaded SLNs as compared to drug suspension.

Table 8.2: Apparent permeability (Papp) and enhancement ratio of AM suspension, AM-SLNs and AM-SMEDDS

	AM suspension	**AM-SLN**	**AM-SMEDDS**
P_{app} (cm/s)	0.89×10^{-6}	6.25×10^{-6}	4.46×10^{-6}
Enhancement ratio	-	7.02	5.01

P_{app} of the AM-SMEDDS and AM-suspension was found to be 4.46×10^{-6} cm/s and 0.89×10^{-6} cm/s, respectively, indicating that SMEDDS showed significantly higher intestinal permeability than drug suspension. The AM-SMEDDS exhibited 5.01 times higher drug permeation than that of AM-suspension at the end of 4 h. It is also reported that nonionic surfactants including Cremophor RH40, Cremophor EL, and Polysorbate 80 are strong CYP3A inhibitors in vitro and in vivo (9,39-41). Hence, enhancement in permeability of AM-SMEDDS might be due to the smaller size of droplets, solubilization improvement and CYP3A inhibitory activity of Cremophor EL which increased drug transport across Caco-2 cells as compared to drug suspension (41,42). Here, inhibitory effect of SMEDDS on intestinal CYP3A may play crucial role in the intestinal absorption of AM.

Thus, the enhancement of AM permeation by encapsulating in SLNs and SMEDDS was verified in vitro using the Caco-2 intestinal cell monolayer.

8.4.5.2 Lurasiodne hydrochloride (LH) loaded SLNs, Lurasiodne hydrochloride loaded SMEDDS and drug suspension

The amount of drug transfer from LH-SLNs, LH-SMEDDS and LH-suspension across Caco-2 monolayer is shown in table 8.3.

Table 8.3: Drug transfer across the Caco-2 cell line for LH-SLNs, LH-SMEDDS and LH suspension

Time (min)	LH suspension	LH-SLNs	LH-SMEDDS
	Amount of drug transfer (mg)	Amount of drug transfer (mg)	Amount of drug transfer (mg)
30	0.002	0.012	0.015
60	0.005	0.041	0.051
120	0.017	0.058	0.078
180	0.021	0.096	0.105
240	0.036	0.140	0.132

The results showed that P_{app} of the LH-SLNs and LH-suspension was found to be 4.46×10^{-6} cm/s and 1.79×10^{-6} cm/s, respectively. The transport of LH-SLNs exhibited 2.50 times higher drug permeation than that of LH-suspension at the end of 4 h. LH-SLNs showed 2.5 times higher intestinal permeation as compared to LH-suspension. This could be due to presence of penetration enhancer, sodium deoxycholate in SLNs which further contributed to increase in permeability of LH loaded SLNs across Caco-2 monolayer.

Table 8.4: Apparent permeability (P_{app}) and enhancement ratio of LH suspension, LH-SLNs and LH-SMEDDS

	LH-DS	LH-SLN	LH-SMEDDS
P_{app} (cm/s)	1.79×10^{-6}	4.46×10^{-6}	3.57×10^{-6}
Enhancement ratio	-	2.50	2.00

P_{app} of the LH-SMEDDS and drug suspension was found to be 3.57×10^{-6} cm/s and 1.79×10^{-6} cm/s, respectively, indicating that LH-SMEDDS showed significantly higher intestinal permeability than LH-suspension (Table 8.4). The LH-SMEDDS exhibited 2 times higher drug permeation than that of LH-suspension at the end of 4 h.

Enhancement in LH loaded SMEDDS can be attributed to nano-droplets, solubilization improvement and CYP3A inhibitory activity of Cremophor EL which increased drug transport across Caco-2 cells as compared to drug suspension (40,41).

8.5 CONCLUSION

Caco-2 cells were selected to form intestinal epithelial cell monolayers to study the related transport mechanisms of the SLNs and SMEDDS crossing the cell monolayers. The results of cell viability assay against Caco-2 cells proved that both SLNs and SMEDDS had low cytotoxicity and were found to be safe for oral administration. The enhanced intracellular uptake of both SLNs and SMEDDS was confirmed by confocal and flow cytometry analysis. The mechanistic study allowed to prove that SLNs transport in Caco-2 cells followed active transport process and endocytosis was proven to be mediated by clathrin and lipid raft/claveole. Thus, all developed lipid based nanoformulations, SLNs and SMEDDS of AM and LH can significantly improve the permeability of both drugs across intestinal epithelial cells, reduce first pass metabolism and improve their oral bioavailability.

8.6 REFERENCES

1. Artursson P, Karlsson J. Correlation between oral drug absorption in humans and apparent drug permeability coefficients in human intestinal epithelial (Caco-2) cells. Biochem Biophys Res Commun. 1991;175(3):880-885.
2. http://www.sgs.nl/~/media/Global/Documents/Technical%20Documents/SGS-Clinical-CACO-2-EN-11.pdf
3. Natoli M, Leoni BD, D'Agnano I, Zucco F, Armando Felsani. Good Caco-2 cell culture practices. Toxicol in Vitro. 2012;26:1243–1246.
4. Gamboa JM, Leong KW. In vitro and in vivo models for the study of oral delivery of nanoparticles. Adv Drug Deliv Rev. 2013;65(6):800–810.
5. Hubatsch I, Ragnarsson EGE, Artursson P. Determination of drug permeability and prediction of drug absorption in Caco-2 monolayers. Nat protoc. 2007;2(9):2111-2119.
6. Beg S, Sharma G, Thanki K, Jain S, Katare OP, Singh B. Positively Charged Self-Nanoemulsifying Oily Formulations of Olmesartan Medoxomil: Systematic Development, In Vitro, Ex Vivo and In Vivo Evaluation. Int J Pharm. 2015;493(1-2):466-482.
7. Shi LL, Cao Y, Zhu XY, Cui JH, Cao QR. Optimization of process variables of zanamivir-loaded solid lipid nanoparticles and the prediction of their cellular transport in Caco-2 cell model. Int J Pharm. 2015;478(1):60-69.
8. Shah MK, Madan P, Lin S. Elucidation of intestinal absorption mechanism of carvedilol-loaded solid lipid nanoparticles using Caco-2 cell line as an in-vitro model. Pharm Dev Technol. 2015;20(7):1-9.
9. Zhao G, Huang J, Xue K, Si L, Li G. Enhanced intestinal absorption of etoposide by self-microemulsifying drug delivery systems: Roles of P-glycoprotein and cytochrome P450 3A inhibition. Eur J Pharm Sci. 2013;50:429–439.
10. Calcagno AM, Ludwig JA, Fostel JM, Gottesman MM, Ambudkar SV. Comparison of drug transporter levels in normal colon, colon cancer, and Caco-2 cells: impact on drug disposition and discovery. Mol Pharmacol. 2006;3(1):87-93.
11. Joshi G, Kumar A, Sawant K. Enhanced bioavailability and intestinal uptake of Gemcitabine HCl loaded PLGA nanoparticles after oral delivery. Eur J Pharm Sci. 2014;60:80-89.

12. Rivolta I, Panariti A, Lettiero B, Sesana S, Gasco P, Gasco MR, Masserini M, Miserocchi G. Cellular uptake of coumarin-6 as a model drug loaded in solid lipid nanoparticles. J Physiol and Pharmacol. 2011;62(1):45-53.
13. Shi LL, Xie H, Lu J, Cao Y, Liu JY, Zhang XX, Zhang H, Cui JH, Cao QR. Positively Charged Surface-Modified Solid Lipid Nanoparticles Promote the Intestinal Transport of Docetaxel through Multifunctional Mechanisms in Rats. Mol Pharm. 2016;13(8):2667–2676.
14. Fenyvesi F, Reti-Nagy K, Bacso Z, Gutay-Toth Z, Malanga M, Fenyvesi E, Szente L, Varadi J, Ujhelyi Z, Feher P, Szabo G, Vecsernyes M, Bacskay I. Fluorescently Labeled Methyl-Beta-Cyclodextrin Enters Intestinal Epithelial Caco-2 Cells by Fluid-Phase Endocytosis. PLoS One. 2014;9(1):1-11.
15. Beloqui A, Solinis MA, Alicia R. Gascon AR, Pozo-Rodriguez AD, Rieux AD, Preat V. Mechanism of transport of saquinavir-loaded nanostructured lipid carriers across the intestinal barrier. J Control Release. 2013;166:115–123.
16. Joshi G, Kumar A, Sawant K. Bioavailability enhancement, Caco-2 cells uptake and intestinal transport of orally administered lopinavir loaded PLGA nanoparticles. Drug Deliv. 2016;23(9):3492-3504.
17. Negi ML, Tariq M, Talegaonkar S. Nano scale self-emulsifying oil based carrier system for improved oral bioavailability of camptothecin derivative by P-Glycoprotein modulation. Colloids Surf B. 2013;111:346– 353.
18. Zhang Z, Gao F, Bu H, Jisheng Xiao, Li Y. Solid lipid nanoparticles loading candesartan cilexetil enhance oral bioavailability: in vitro characteristics and absorption mechanism in rats. Nanomed Nanotech Biol Med. 2012;8:740–747.
19. Jose S, Anju SS, Cinu TA, Aleykutty NA, Thomas S, Souto EB. In vivo pharmacokinetics and biodistribution of resveratrol-loaded solid lipid nanoparticles for brain delivery. Int J Pharm. 2014;474:6–13.
20. Yin YM, Cui FD, Mu CF, Choi MK, Kim JS, Chung SJ, Shim CK, Kim DD. Docetaxel microemulsion for enhanced oral bioavailability: Preparation and in vitro and in vivo evaluation. J Control Release. 2009;140:86–94.
21. Doktorovova S, Souto EB, Silva AM. Nanotoxicology applied to solid lipid nanoparticles and nanostructured lipid carriers – A systematic review of in vitro data. Eur J Pharm Biopharm. 2014;87:1–18.

22. Aillon KL, Xie Y, El-Gendy N, Berkland CJ, Forrest ML. Effects of nanomaterial physicochemical properties on in vivo toxicity. Adv Drug Deliv Rev. 2009;61:457–466.
23. Arora S, Rajwade JM, Paknikar KM. Nanotoxicology and in vitro studies: The need of the hour. Toxicol Appl Pharmacol. 2012;258:151–165.
24. Chai GH, Xu Y, Chen SQ, Cheng B, Hu FQ, You J, Du YZ, Hong Yuan H. Transport Mechanisms of Solid Lipid Nanoparticles across Caco-2 Cell Monolayers and their Related Cytotoxicology. ACS Appl Mater Interfaces. 2016;8(9):5929-5940.
25. Sha X, Yan G, Wu Y, Li J, Fang X. Effect of self-microemulsifying drug delivery systems containing Labrasol on tight junctions in Caco-2 cells. Eur J Pharm Sci. 2005;24:477–486.
26. Wahlang B, Pawar YB, Bansal AK.Identification of permeability-related hurdles in oral delivery of curcumin using the Caco-2 cell model. Eur J Pharm Biopharm. 2011;77:275–282.
27. Gursoy N, Garrigue JS, Razafindratsita A, Lambert G, Benita S. Excipient Effects on In Vitro Cytotoxicity of a Novel Paclitaxel Self-Emulsifying Drug Delivery System. J Pharm Sci. 2003;92(12):2411-2418.
28. Win KY, Feng SS. Effects of particle size and surface coating on cellular uptake of polymeric nanoparticles for oral delivery of anticancer drugs. Biomaterials. 2005;26:2713–2722.
29. Lai Y, Chiang PC, Blom JD, Li N, Shevlin K, Brayman TG, Hu Y, Selbo JG, Hu LG. Comparison of In vitro Nanoparticles Uptake in Various Cell Lines and In vivo Pulmonary Cellular Transport in Intratracheally Dosed Rat Model. Nanoscale Res Lett. 2008;3:321–329.
30. Ji H, Tang J, Li M, Ren J, Zheng N, Wu L. Curcumin-loaded solid lipid nanoparticles with Brij78 and TPGS improved in vivo oral bioavailability and in situ intestinal absorption of curcumin. Drug Deliv. 2016;23(2):549-470.
31. Guo Y, Luo J, Tan S, Otieno BO, Zhang Z. The applications of Vitamin E TPGS in drug delivery. Eur J Pharm Sci. 2013;49(2):175-186.
32. Kolliparan S, Gandhi RK. Pharmacokinetic aspects and in vitro–in vivo correlation potential for lipid-based formulations. Acta Pharm Sin B. 2014;4(5):333–349.

33. Liang M, Lin I, Whittaker MR, Minchin RF, Monteiro MJ, Toth I. Cellular Uptake of Densely Packed Polymer Coatings on Gold Nanoparticles. ACS Nano. 2010;4(1):403-413.
34. Roger E, Lagarce F, Garcion E, Benoit JP. Lipid nanocarriers improve paclitaxel transport throughout human intestinal epithelial cells by using vesicle-mediated transcytosis. J Control Release. 2009;140:174–181.
35. Chen C, Fan T, Jin Y, Zhou Z, Yang Y, Zhu X, Zhang Z, Zhang Q, Huang Y. Orally delivered salmon calcitonin-loaded solid lipid nanoparticles prepared by micelle–double emulsion method via the combined use of different solid lipids. Nanomedicine. 2013;8(7):1085–1100.
36. Ivanov AI. Pharmacological Inhibition of Endocytic Pathways: Is It Specific Enough to Be Useful? Methods in Molecular Biology. Humana Press, Totowa, NJ. 15-33.
37. Kou L, Sun J, Zhai Y, He Z. The endocytosis and intracellular fate of nanomedicines: Implication for rational design. Asian J Pharm Sci. 2013;8:1-10.
38. Zhang BS, Li J, Lykotrafitis G, Bao G, Suresh S. Size-Dependent Endocytosis of Nanoparticles. Adv Mater. 2009;21:419–424.
39. Lim SK, Banerjee A, Onyuksel H. Improvement of drug safety by the use of lipid-based nanocarriers. J Control Release. 2012;163:34–45.
40. Lu Y, Qi J, Wei Wu W. Absorption, Disposition and Pharmacokinetics of Nanoemulsions. Curr Drug Metab. 2012;13:396-417.
41. Rege BD, Kao JPY, Polli JE. Effects of nonionic surfactants on membrane transporters in Caco-2 cell monolayers. Eur J Pharm Sci. 2002;16:237–246.
42. Ke Z, Hou X, Jia XB. Design and optimization of self-nanoemulsifying drug delivery systems for improved bioavailability of cyclovirobuxine D. Drug Des Dev Ther. 2016:10;2049–2060.